Investigation of the Initial Reactions of the Calcote Mechanism for Soot Formation

Helge Egsgaard

Department of Combustion Research, Risø National Laboratory, DK-4000 Roskilde, Denmark

The first three reactions of the Calcote mechanism for soot formation, that is, $C_3H_3^+ + C_2H_2 \rightarrow C_5H_5^+$, $C_5H_5^+ \rightarrow C_5H_3^+ + H_2$, and $C_5H_3^+ + C_2H_2 \rightarrow C_7H_5^+$, have been studied based on chemi-ions withdrawn directly from a premixed methane–oxygen flame by supersonic molecular beam sampling. The first reaction is reversible and involves the formation of a specific encounter complex sensitive to pressure and ion kinetic energy. The second reaction appears to require large amounts of internal energy in the $C_5H_5^+$ ion to proceed. The third reaction is reversible; however, in contrast to the initiating reaction, the $C_5H_3^+$ ion formed from the $[C_7H_5^+]^*$ complex exhibits a much lower reactivity. The conclusions are based on ion-molecule reactions as well as collision activation mass spectrometry of isolated chemi-ions. In addition, the product distributions as functions of pressure and ion kinetic energy were studied. (*J Am Soc Mass Spectrom* 1996, 7, 559–564)

The enhanced ionization of flames has been a challenge to the combustion chemist for more than five decades [1]. However, in the late 1950s the chemical origin of the ions was firmly established [2]. Thus, the reaction between the parent methylidyne, CH, and atomic oxygen appears to be of general significance [1, 3, 4]. This reaction leads to a highly excited formyl radical and, subsequently, by expulsion of an electron, to the formyl cation. Proton transfer from the latter to other flame constituents as well as secondary ion–molecule reactions gives rise to a rich and complex ion chemistry within the flame:

$$CH + O \rightarrow CHO^* \rightarrow CHO^+ + e^-$$

The ionic mechanism for soot formation remains unique in the sense that the ionic reactants seem to play here a dominant role in a common combustion process. It should, however, be noted that there are essentially two current mechanisms proposed for soot formation in flames [5, 6]. The most widely accepted mechanism is based on free radical reactions and the other on an ionic mechanism [5].

Both models for soot formation are well documentated with respect to their kinetic aspects, and the mechanisms may indeed operate in concert. The ionic mechanism, however, gains strong support by the direct observation of the ionic species at the molecular as well as particulate level [5]. In addition, soot formation can be influenced by electric fields and charged additives [5, 7, 8]. Finally, it should be noted that some exotic flames, for example, CS_2/O_2, do not reveal classical chemi-ionization; the same flames are virtually without sooting properties [5].

Very recently we have demonstrated the application of tandem mass spectrometry to chemi-ions based on supersonic molecular beam sampling [9, 10]. This methodology gives unique possibilities to characterize a given ion based on collision activation mass spectrometry as well as to study the reactivity of the isolated chemi-ion.

Based on this strategy we are in a position to withdraw the highly reactive ionic intermediates of relevance to soot formation *directly* from the flame [11]. Thus, the studies on the reactivity of chemi-ions are experiments that involve the species actually present in the flame and conceivable reactants under highly controlled conditions. We report here on the first three stages of the ionic reaction model for soot formation, that is, $C_3H_3^+ + C_2H_2 \rightarrow C_5H_5^+$, $C_5H_5^+ \rightarrow C_5H_3^+ + H_2$, and $C_5H_3^+ + C_2H_2 \rightarrow C_7H_5^+$ based on isolated chemi-ions.

Experimental

The premixed flame was burned on a simple quartz burner (CH_4; 1.0 L/min; O_2; 1.0 L/min) as previously described [9–13].

The ions were sampled by a high temperature supersonic molecular beam inlet and analyzed on a custom built triple quadrupole mass spectrometer. The instrument is based on a modified high temperature sampling front end that utilizes the Plasma-Quad technology (VG Elemental, Middlewich, Cheshire, England) and a triple-quadrupole mass spectrometer based on the API-200 series (VG Gas Analysis) [9, 10].
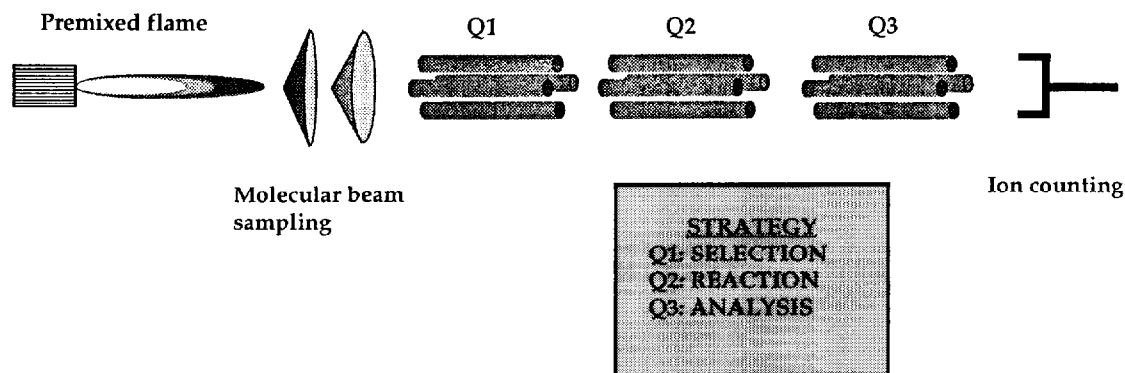
Figure 1. System layout.

Complete mass spectra were obtained by keeping the first and second quadrupoles (Q1 and Q2) in the rf-only mode and scanning the third quadrupole (Q3).

In the tandem mass spectrometry experiments the chemi-ion of interest, for example, $C_3H_3^+$, was selected by Q1, and after collisions in the collision cell (Q2), the ionic products were analyzed by the third quadrupole (Q3). Collision activation mass spectra were the results of 5-eV collisions that utilized argon as a collision partner.

The ion–molecule reactions were studied by admission of acetylene and D_2-acetylene, respectively, to the collision cell. The translational energy of the reacting ions was kept low, that is, < 0.5 eV. The experimental setup as well as the strategy for the study of ion-molecule reactions are outlined in Figure 1.

Figure 2. The ionic model of soot formation (ref. 5).

Results and Discussion

The ionic mechanism is initiated by the chemi-ion $C_3H_3^+$, that is, the propargylic cation, which rapidly grows by the addition of acetylene. The eventual products become the incipient soot particles, charged or neutral dependent on electron recombination. The classical ionic mechanism as championed by Calcote is given in Figure 2 [5].

The major difference between the ionic and free radical mechanisms is found in the details of the first stages of the reactions and, hence, in well defined reactions on the molecular level.

The CH_4/O_2 flame is one of the most widely studied with a maximum of approximately 4×10^{10} ions/cm^3 for a fuel-lean flame [4, 12]. In the reaction zone the $C_3H_3^+$ chemi-ion is by far the most abundant, see Figure 3. In addition, the ions to be considered in the following stages of the ionic mechanism for soot formation are of sufficient intensity to facilitate the tandem mass spectrometry experiments. The chemi-ions of relevance to soot formation are indicated in Figure 3.
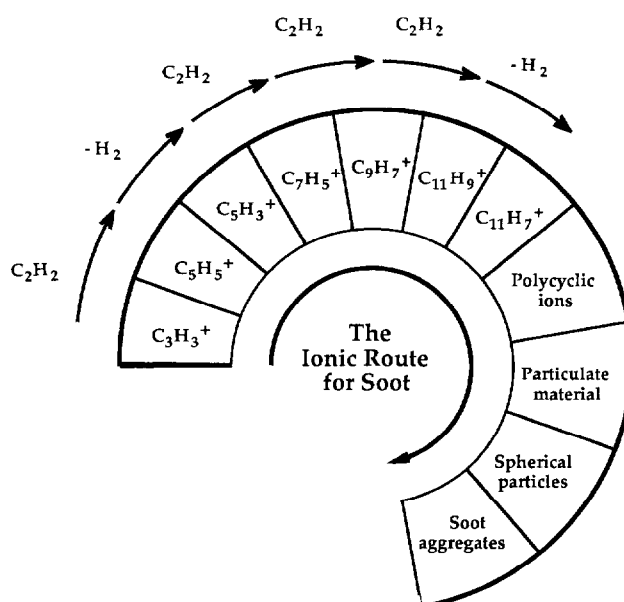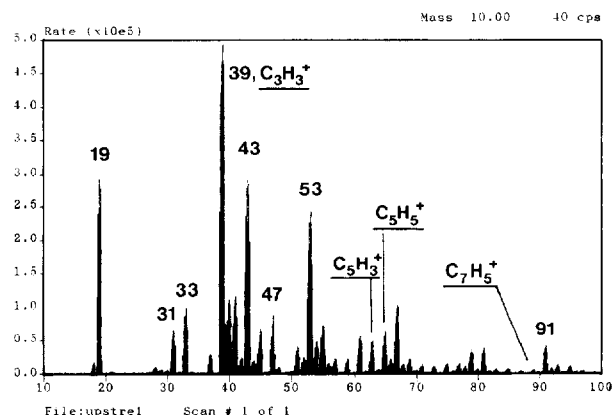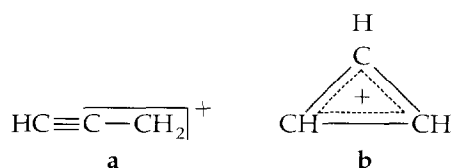

Figure 3. Mass spectrum of the ions sampled from the reaction zone of a premixed methane–oxygen flame. The ions that participate directly in the ionic soot mechanism are indicated on the figure.

## *The Primary Reaction:* $C_3H_3^+ + C_2H_2 \rightarrow C_5H_5^+$

The primary reaction, that is, the addition of acetylene to $C_3H_3^+$, previously has been studied experimentally by ion cyclotron resonance (ICR) mass spectrometry [14, 15]. In addition, the reaction has been studied in a higher pressure regime by ion trap mass spectrometry [16], triple quadrupole mass spectrometry [17], and selected ion flow tube (SIFT) methodology [18, 19]. These studies have unambiguously demonstrated a very large difference in reactivity of the two $C_3H_3^+$ isomers:

$$HC{\equiv}\overline{C{-}CH_2}]^+ \qquad CH\overline{\overset{\overset{\displaystyle H}{\overset{\displaystyle C}{\diagup{+}\diagdown}}}{\rule{0pt}{0pt}}}CH$$
$$\text{a} \qquad\qquad\qquad \text{b}$$

The linear propargylic structure **a** is orders of magnitude more reactive than the cyclopropenyl cation **b** [14–19]. The latter is, however, thermodynamically favored by as much as 104 kJ/mol ($\Delta_f H$ l-$C_3H_3^+$; 1179 kJ/mol and $\Delta_f H$ c-$C_3H_3^+$; 1075 kJ/mol [20]). Thus, it has been estimated that the propargylic form contributes to only approximately 1% of the $C_3H_3^+$ ions present in the flame [21]. The calculation has been supported by more recent experiments based on deuterium labeling and a statistical evaluation of the intramolecular distribution of the label [13]. Thus, only a minor part of the $C_3H_3^+$ chemi-ions can be expected to enter the soot cycle.

Figure 4 shows the mass spectra following the reaction of the $C_3H_3^+$, m/z 39, chemi-ion with C_2H_2 and C_2D_2. The primary adduct $[C_5H_5^+]^*$, m/z 65, is directly observed (Figure 4a) in contrast to what has been reported previously in the ICR experiments [14, 15] and the intensity is improved greatly compared with the ion trap experiments [16]. The very high deuterium content in the encounter complex (m/z 65–70) and C_3-species (m/z 39–42) observed in the C_2D_2 experiments (Figure 4b) are in excellent agreement with the reversibility of the reaction as disclosed previously [14–16].

It is an unique feature of the reaction that when the C_5 complex breaks up, the $C_3H_3^+$ ion is formed in a mixture of the **a** and **b** isomers [14–16]. The reaction causes a distribution of the isotopic label (deuterium or ^{13}C) that originates from acetylene in the products, that is, the ionic C_3 species and acetylene [14–16].

$$l\text{-}C_3H_3^+ + C_2H_2 \atop c\text{-}C_3H_3^+ + C_2H_2} \Big\rangle [C_6H_5^+]^* \rightarrow \text{products}$$
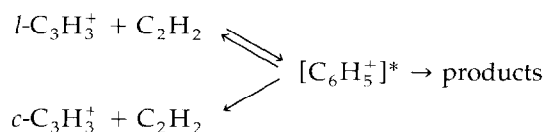
This leads ultimately to the very high deuterium content of the C_5 complex as well as a significant deu-
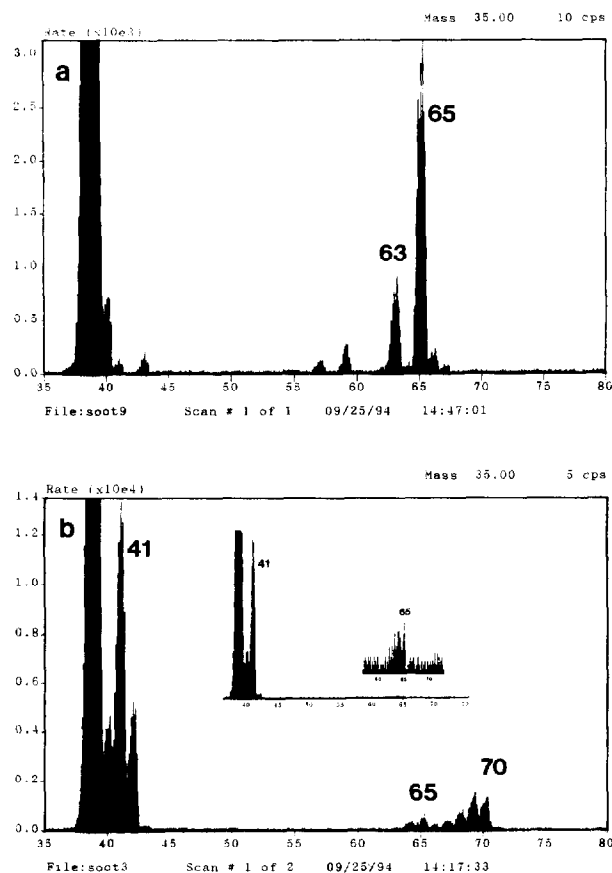

Figure 4. Ion distribution after reaction of the $C_3H_3^+$ chemi-ion with (a) acetylene and (b) D_2-acetylene. The $C_3H_3^+$ chemi-ion (m/z 39) was selected by the first quadrupole and, following reactive collisions in the second quadrupole, the ionic products were analyzed by the final quadrupole. The ion distribution after reaction of the $C_3H_3^+$ chemi-ion with D_2-acetylene that utilized 5-eV ion kinetic energy is shown as an insert in (b).

terium content in the C_3 ions (cf. Figure 4b). The isotopically labeled C_3 ions seems to be due mainly to the formation of a nonreactive cyclopropenyl cation.

The reactions of $C_3H_3^+$ with acetylene and deuteroacetylene previously have been studied by reaction kinetic modeling and then compared to ICR experiments [14]. The reactions were successfully modeled to yield a nearly statistical distribution of deuterium and a rather large kinetic isotope effect [14]. The predominance of $C_3HD_2^+$, m/z 41, after the reaction of the $C_3H_3^+$ chemi-ion with deuteroacetylene (Figure 4b) cannot be rationalized in terms of this generalized model. To account for this, a specific formation of the encounter complex $[C_5H_5^+]^*$ has to be invoked. The structural $C_5H_5^+$ isomers have been studied by high level molecular orbital (MO) calculation [22]. The most stable structure was found to be the vinyl-cyclopropenyl cation **c**. However, only moderate energy differences, that is, 10–30 kcal/mol, were found

between a number of conceivable isomers [22]:
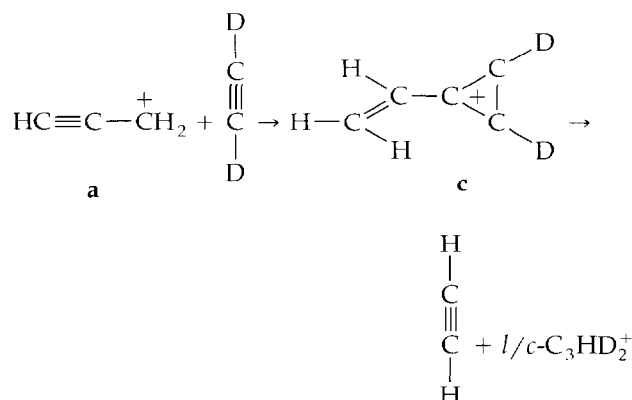
The suggested preference for the $C_5H_5^+$ isomer **c** may well be due to a significantly lower rovibrational energy level of the reacting $C_3H_3^+$ chemi-ion caused by the adiabatic sampling from the flame. Thus, we calculate a temperature of approximately 200 K at the point of freeze-in [10]. This is obviously much lower than generally encountered in ion–molecule experiments and in this context it should be noted that ion trap experiments apparently involve unusually hot ions, that is, with ion temperatures on the order 600–800 K [23, 24].

The observation of the $C_5H_5^+$ product ion is the result of an efficient collisional deactivation of the encounter complex. However, the stabilization of the latter may be influenced by other factors, for example, the ion kinetic energy.

From an analytical point a moderate to high kinetic energy is to be preferred. However, the bimolecular reactions obviously benefit from near thermal energies. In the present studies translational energy is in general kept low, that is, ≤ 0.5 eV. Raising the energy has a pronounced influence on the product distribution. Figure 4b includes as an insert the resulting mass spectrum based on 4.5 eV reactant ions. The virtual absence of the encounter complex (m/z 66–70) is immediately apparent—only a very weak signal for $C_5HD_2^+$, m/z 65, which corresponds to the secondary reaction $C_5H_5^+ \rightarrow C_5H_3^+ + H_2$, may be traced (Figure 4b). The isotopic pattern of the C_3 ions indicates, on the other hand, that the complex does form as evidenced by, for example, the abundant m/z 41, $C_3HD_2^+$. Thus, the encounter complex breaks up before collisional deactivation takes place as a result of a possible weak, but sufficient, transformation of translational energy to rovibrational energy, which causes a much more rapid fragmentation of the encounter complex than observed near thermal kinetic energies.

The isotopic pattern of the C_3 ions reveals only minor changes, and these are apparently sensitive to the ion kinetic energy. Thus, the ions at the high mass end, for example, m/z 42, are of lower intensity. This may tentatively be explained by an increasing ratio of

the cyclo–linear isomers formed from the encounter complex at the higher impact energies.

The Second Stage: $C_5H_5^+ \rightarrow C_5H_3^+ + H_2$

The product ion $C_5H_3^-$ (m/z 63) considered in the second stage of the ionic mechanism for soot formation, that is, $C_5H_5^+ \rightarrow C_5H_3^- + H_2$, can be observed already in the primary reaction, see Figure 4. The ratio $C_5H_3^+/C_5H_5^-$ given by the intensity ratio of the m/z 63 and 65 ions was found to be highly dependent on the pressure in the collision cell. In Table 1 the ratio $C_5H_3^+/C_5H_5^+$ is a function of the pressure measured in the quadrupole housing. It appears that the ratio decreases approximately linearly as the pressure is raised from 2.3 to 6.6 10^{-5} mbar (Table 1). Thus, the formation of $C_5H_3^+$ appears to be highly dependent on the internal energy of the $C_5H_5^+$.

An investigation of the $C_5H_5^+$ chemi-ion by collision activation, that is, by approximately 5-eV collisions by using argon as an inert collision partner, leads only to the loss of acetylene with virtually no loss of H or H_2. Thus, it can be concluded that the formation of $C_5H_3^+$ by the formal loss of H_2 has a higher critical energy than the elimination of acetylene from $C_5H_5^+$. The formation of the $C_5H_3^+$, m/z 63, in the flame in quantities sufficient for soot formation has, hence, to be sought in the pressure and temperature duality favoring deactivation and activation, respectively.

The Third Stage: $C_5H_3^+ + C_2H_2 \rightarrow C_7H_5$

The third reaction, $C_5H_3^+ + C_2H_2 \rightarrow C_7H_5$ shows some resemblance to the initial reaction between $C_3H_3^-$ and acetylene. Figure 5 shows the mass spectra that result from the reaction of $C_5H_3^+$ with both acetylene and deuteroacetylene. The primary adduct $C_7H_5^+$, m/z 89, is immediately recognized in Figure 5a. The experiment that utilizes D_2-acetylene unambiguously discloses the reversibility of the reaction because significant amounts of deuterium are incorporated in the C_5-precursor ion. Thus, the formation of m/z 64 and 65 corresponds to $C_5H_2D^+$ and $C_5HD_2^+$, respectively (cf. Figure 5b).

The adduct is characterized by predominance of $C_7H_3D_2^+$, m/z 91. The high abundance of the D_2-isotopomer indicates that the reaction differs markedly from that observed from the analogous reaction with $C_3H_3^+$. Thus, it can be concluded that major part of the $C_5H_3^+$ ions formed from the $[C_7H_5^+]^*$ adduct are non-reactive in contrast to the 2:1 ratio of reactive and nonreactive species returned from the $[C_5H_5^+]^*$ complex [16]. This is in accordance with previous ICR experiments on $C_5H_3^+$ and $C_5H_5^+$ ions selected from various precursors [25].

The third reaction shows the same dependence on pressure as the initial reaction. Thus, the intensity of the primary adduct $C_7H_5^+$ increases with increasing

Table 1. Pressure dependence of the reaction
$$[C_5H_5^+]^* \rightarrow C_5H_3^+ + H_2$$

Pressure[a] $\times 10^{-5}$ (mbar)	Intensity ratio of $C_5H_3^+/C_5H_5^+$ (m/z 63 and 65, respectively)
2.3	0.30
3.8	0.23
6.6	0.17

[a] The pressure is measured in the quadrupole housing, that is, outside the collision cell.
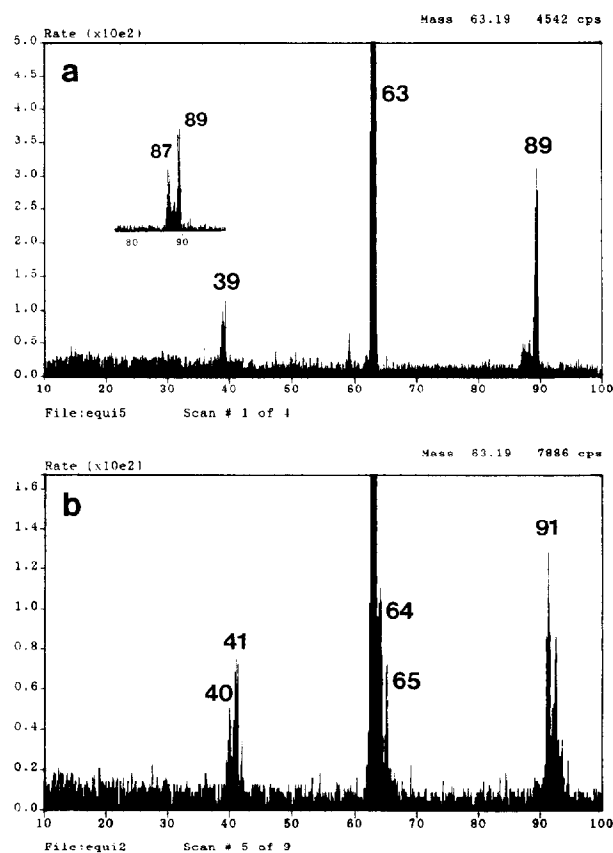

Figure 5. Ion distribution after reaction of the $C_5H_3^-$ chemi-ion with (a) acetylene and (b) D_2-acetylene. The insert in (a) shows the distribution at the high mass end at low pressure. The $C_5H_3^+$ chemi-ion (m/z 63) was selected by the first quadrupole and, following reactive collisions in the second quadrupole, the ionic products were analyzed by the final quadrupole.

pressure in the collision cell. The intensity of the adduct, $C_7H_5^+$ and the next product at m/z 87 ($[C_7H_5^+]^* \rightarrow C_7H_3^+ + H_2$) becomes comparable at very low pressure (quadrupole housing $\approx 2.5 \times 10^{-5}$ mbar); see Figure 5a.

Equilibrium between polyynic ions, for example, the $C_{3+2n}H_3^+$ series and neutral alkynes has previously been suggested based on the characteristic patterns in which the ions appear and their C/O dependence [26, 27]. Assuming the partial equilibrium

$$C_{3+2n}H_3^+ + C_4H_2 \leftrightarrows C_{3+2(n+1)}H_3^+ + C_2H_2$$
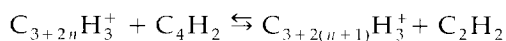
the enthalpies of formation of the polyynic flame ions were calculated succesfully [26, 27]. This kind of equilibrium is also in clear evidence in our experiments. Thus, the formation of $C_3H_3^+$ and its isotopomers correspond to the elimination of diacetylene from the C_7 species formed from the ion-molecule reaction between $C_5H_3^+$ and acetylene (cf. Figure 5) and may be regarded as an experimental proof of the proposed partial equilibrium. The $C_3H_3^+$ species are predominant at low pressure, which points to some, however minor, energy requirements for formation.

Finally, it should be noted that the formation of the apparent nonreactive $C_5H_3^+$ species indicates that not all $C_5H_3^+$ chemi-ions can be expected to enter the soot mechanism. The high flame temperature may, on the other hand, enhance the reactivity of the $C_5H_3^+$ ion as well as the equilibrium between polyynic ions and alkynes.

Based on the experiments discussed, the first reactions of the Calcote mechanism for soot formation can be rationalized as follows:
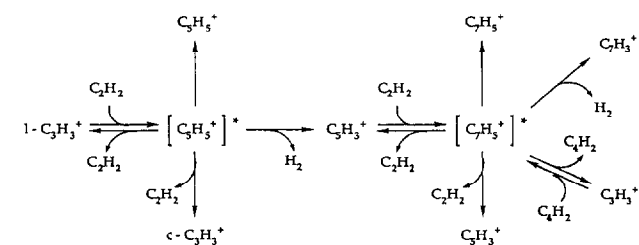
Conclusion

It has been demonstrated that chemi-ions withdrawn *directly* from a premixed flame by supersonic molecular beam sampling can be used advantageously in investigations of reactions related to the ionic mechanism for soot formation.

The first three reactions of the Calcote mechanism for soot formation, that is, $C_3H_3^+ + C_2H_2 \rightarrow C_5H_5^+$, $C_5H_5^+ \rightarrow C_5H_3^+ + H_2$, and $C_5H_3^+ + C_2H_2 \rightarrow C_7H_5^+$ have successfully been studied. The first reaction was found to be reversible and involves the formation of a specific encounter complex sensitive to pressure and ion kinetic energy. The second reaction appears to require large amounts of internal energy in the $C_5H_5^+$ ion in order to proceed. The third reaction is reversible; however, in contrast to the initiating reaction, the $C_5H_3^+$ ion formed from the $[C_7H_5^+]^*$ complex exhibits a much lower reactivity. In addition the investigation of the third reaction strongly supports the partial equilibrium between polyynic ions and simple alkynes in flames.

References

1. Hayhurst, A. N. H.; Jones, H. R. N. *J. Chem. Soc. Faraday Trans. 2*, **1987**, *83*, 1.
2. Calcote, H. F. *Proceedings of the Eighth International Symposium on Combustion*; 1962; p 184.

3. Goodings, J. M.; Tanner, S. D.; Bohme, D. K. *Can. J. Chem.* **1982**, *60*, 2766.

4. Bohme, D. K. In *Kinetics of Ion–Molecule Reactions*; Ausloos, P. J., Ed.; Plenum: New York, 1979; p 323.

5. Calcote, H. F. *Combust. Flame* **1981**, *42*, 215.

6. Calcote, H. F.; Keil, D. G. *Pure and Appl. Chem.* **1990**, *62*, 815.

7. Mayo, P. J.; Weinberg, F. J. *Proc. Roy. Soc. London* **1970**, *319*, 351.

8. Goodings, J. M.; Graham, S. M.; Karellas, N. S. *Int. J. Mass Spectrom. Ion Processes* **1986**, *69*, 343.

9. Egsgaard, H.; Thomsen, M. S.; Larsen, E. *Proceedings of 42nd ASMS Conference on Mass Spectrometry Allied Topics*; 1994; p 1091.

10. Egsgaard, H.; Carlsen, L. *Chem. Phys. Lett.* **1995**, *236*, 78.

11. Egsgaard, H. *Proceedings of 43nd ASMS Conference Mass Spectrometry Allied Topics*; 1995; p 78.

12. Egsgaard, H.; Carlsen, L. *J. Anal. Appl. Pyrol.* **1993**, *25*, 361.

13. Egsgaard, H.; Larsen E., Kristensen; L. V.; Solgaard, P; Carlsen, L. *Analyst* **1994**, *119*, 605.

14. Wiseman, F. L.; Ozturk, F.; Zerner; M. C.; Eyler, J. R. *Int. J. Chem. Kinet.*. **1990**, *22*, 1189.

15. Ozturk, F.; Baykut, G.; Moini, M.; Eyler, J. R. *J. Phys. Chem.* **1987**, *91*, 4360.

16. Moini, M. *J. Am. Soc. Mass Spectrom.* **1992**, *3*, 631.

17. Fetterolf D. D.; Yost, R. A.; Eyler, J. R. *Org. Mass Spectrom.* **1984**, *19*, 104.

18. McEvann, M. J.; McConnell C. L.; Freemann C. G.; Anicich, G. *J. Phys. Chem.* **1994**, *98*, 5068.

19. Smith, D.; Adams, N. G. *Int. J. Mass Spectrom. Ion Phys.* **1987**, *76*, 307.

20. Lias, S. G.; Bartmess, J. E.; Liebman, J. F.; Holmes, J. L.; Levin, R. G.; Mallard, W. G. *J. Phys. Chem. Ref. Data* **1988**, *17*, Suppl. 1.

21. Smyth, K. C.; Lias, S. G.; Ausloos, P. *Combust. Sci. Technol.* **1982**, *28*, 147.

22. Feng, J.; Leszczynski, J.; Weiner, B.; Zerner, M. C. *J. Am. Chem. Soc.* **1989**, *111*, 4648.

23. Harrison, A.G. *Chemical Ionization Mass Spectrometry*, 2nd ed.; CRC Press; Boca Raton, 1992; p 59.

24. Nourse, B. D.; Kenttämaa, H. I. *J. Phys. Chem.* **1990**, *94*, 5809.

25. Ozturk, F.; Moini, M.; Brill, F. W.; Eyler, J. R.; Buckley, T. J.; Lias, S. G.; Ausloos, P. J. *J. Phys. Chem.* **1989**, *93*, 4038.

26. Michaud, P.; Delfau J. L.; Barassin, A. *18th International Symposium on Combustion*; Pittsburgh, PA; 1981; p 443.

27. Gerhardt, Ph.; K. H. Homann, *J. Phys. Chem.*, **1990**, *94*, 5381.